Quantum non-Markovian Langevin formalism for heavy ion reactions near the Coulomb barrier

V. V. Sargsyan,[1] Z. Kanokov,[1,2] G. G. Adamian,[1,3] and N. V. Antonenko[1]
[1]*Joint Institute for Nuclear Research, RU-141980 Dubna, Russia*
[2]*National University, 700174 Tashkent, Uzbekistan*
[3]*Institute of Nuclear Physics, 702132 Tashkent, Uzbekistan*
(Received 5 July 2007; revised manuscript received 4 October 2007; published 19 February 2008)

The generalized Langevin approach is suggested to describe the capture inside of the Coulomb barrier of two heavy nuclei at bombarding energies near the barrier. The equations of motion for the relative distance (collective coordinate) between two interacting nuclei are consistent with the generalized quantum fluctuation-dissipation relations. The analytical expressions are derived for the time-dependent non-Markovian microscopic transport coefficients for the stable and unstable collective modes. The calculated results show that the quantum effects in the diffusion process increase with increasing friction or/and decreasing temperature. The capture probability inside of the Coulomb barrier is enhanced by the quantum noise at low energies near the barrier. An increase of the passing probability with dissipation is found at sub-barrier energies.

DOI: 10.1103/PhysRevC.77.024607 PACS number(s): 25.70.Jj, 24.10.−i, 24.60.−k

I. INTRODUCTION

Heavy-ion fusion dynamics at energies near the Coulomb barrier has been the object of many experimental and theoretical studies [1–13]. The diffusion Fokker-Planck equation and the system of stochastic Langevin equations have been applied [2,3,5,6,8,13] to the description of the dynamics of fusion and deep-inelastic reactions. The most of investigations deal with a classical treatment in which the friction and diffusion coefficients are related through the classical fluctuation-dissipation relation. The capture process has been simply modeled by classical equations of motion with friction term or by a thermal diffusion over the potential barrier. A classical treatment of dynamical fluctuations is restricted by the Markovian limit. Because the curvature $\hbar\tilde{\omega} \approx$ (1–3) MeV of the Coulomb barrier is larger then the nuclear temperature in the entrance phase of reaction, it is natural to expect the importance of the quantum statistical effect in the capture process. The importance of dynamical quantum fluctuations in the description of the mass and charge distributions of the products of deep inelastic heavy-ion collisions has been mentioned in Refs. [2,3,5,6,8]. The coupling of relative motion with the internal degrees of freedom of the colliding nuclei can be organized to decrease the dissipation rate and enhance the penetration of the Coulomb barrier that is necessary to explain the experimental data on the sub-barrier fusion [11,12].

If the relative motion of two interacting nuclei is rather fast, a colored noise and nonlocal dissipation can be assumed. In this case, the transport coefficients can be strongly modified by memory effect, especially at low temperatures and large damping [14–18].

The present article is an effort to include the quantum effects of fluctuations and dissipations in the treatment of the capture process. We consider the model in which the Coulomb barrier is represented by an inverted oscillator. We address the dynamics of damped collective modes in terms of the first and second moments with the non-Markovian time-dependent transport coefficients. The generalized fluctuation-dissipation relations contain the influence of quantum effects both on the transport coefficients and on the collective motion. It should be noted that there exist investigations [18–26] of the classic and quantum collective motion in an inverted oscillator related with the processes of capture and decay. The consideration of time-dependent quantum diffusion coefficients that govern the dynamics of the second moments for both the stable mode and the unstable mode is still insufficient.

The generalized quantum Langevin equations for the collective coordinate of the relative distance between the interacting nuclei and the quantum fluctuation-dissipation relations are derived in Sec. II A in the case of the general coupling between the collective coordinate and the internal subsystem consisting of the fermionic nucleon degrees of freedom. Using the solution of these Langevin equations, the equations of motion for the first and second moments, which incorporate the quantum statistical effects in terms of time-dependent non-Markovian transport coefficients, are derived in Sec. II B for harmonic and inverted oscillators. In Sec. III the explicit expressions for the microscopic time-dependent transport coefficients are presented in the case of linear coupling in coordinate between the collective and internal subsystems. The numerical calculations of the diffusion coefficients for the stable and unstable collective modes are given in Sec. IV A. The role of quantum statistical effects in the passing probability of the parabolic potential barrier is studied in Sec. IV B.

II. GENERALIZED NON-MARKOVIAN QUANTUM LANGEVIN APPROACH

A. Quantum equations of motion

We consider the dynamics of the heavy-ion fusion reactions at energies near the Coulomb barrier starting from the entrance channel until the formation of the touching configuration. For simplicity, we describe this dynamics in terms of a single collective variable: the relative distance R between the colliding nuclei. It is convenient to represent the Hamiltonian

H of the total system in the form [5,7,8,27,28]

$$H = H_{\rm rel} + H_{\rm in} + H_{\rm int}, \tag{1}$$

where $H_{\rm rel}$, $H_{\rm in}$, and $H_{\rm int}$ are the Hamiltonians of the collective subsystem, the intrinsic nucleonic degrees of freedom, and the coupling of the relative motion to the internal motion, respectively. The collective Hamiltonian

$$H_{\rm rel} = \frac{P^2}{2\mu} + U(R) \tag{2}$$

of relative motion is the sum of the kinetic energy and the interaction potential $U(R)$ of colliding nuclei. Here, P is the conjugate momentum, and μ is the reduced mass. The single-particle Hamiltonian can be written as:

$$H_{\rm in} = \sum_i \varepsilon_i a_i^+ a_i, \tag{3}$$

where ε_i are the energies of the unperturbed single-particle states "i" of the projectile and target. The intrinsic nucleonic degrees of freedom are expressed through the nucleon creation a_i^+ and annihilation a_i operators. The coupling Hamiltonian [8,27]

$$H_{\rm int} = \sum_{i,k} V_{ik}(R, P) a_i^+ a_k \tag{4}$$

corresponds to the particle-hole transitions between the single-particle levels in one of the nuclei under the influence of the partner nucleus and to the transitions of the nucleons from nucleus to nucleus because of the action of the mean field of the dinuclear system. Information about the evolution of the dinuclear system can be obtained by solving the equation of motion for the single-particle degrees of freedom $n_i(t) = n_{ii}(t) = a_i^+(t)a_i(t)$ and $n_{ik}(t) = a_i^+(t)a_k(t)$

$$\begin{aligned} i\hbar\frac{dn_i(t)}{dt} &= [H, n_i(t)] = \sum_k \{V_{ki}(R(t), P(t))n_{ki}(t) \\ &\quad - V_{ik}(R(t), P(t))n_{ik}(t)\}, \end{aligned} \tag{5}$$

$$\begin{aligned} i\hbar\frac{dn_{ik}(t)}{dt} &= [H, n_{ik}(t)] = \hbar\omega_{ik}n_{ik} + V_{ki}(R(t), P(t)) \\ &\quad \times [n_k(t) - n_i(t)], \end{aligned} \tag{6}$$

where $\omega_{ik} = (\varepsilon_i - \varepsilon_k)/\hbar$. In Eq. (6) we make the simplification (random-phase approximation)

$$\sum_{k'} V_{k'i}n_{k'k} - \sum_{i'} V_{ki'}n_{ii'} \approx V_{ki}(n_k - n_i).$$

Then substituting the solution

$$\begin{aligned} n_{ik}(t) &= e^{i\omega_{ki}(t-t_0)}n_{ik}(t_0) + \frac{1}{i\hbar}\int_{t_0}^{t} dt' e^{i\omega_{ki}(t-t')}V_{ki}(R(t'), P(t')) \\ &\quad \times [n_k(t') - n_i(t')] \end{aligned} \tag{7}$$

of Eq. (6) in Eq. (5), we obtain the equation for the dynamical occupation numbers $n_i(t)$:

$$\begin{aligned} \frac{dn_i(t)}{dt} &= \frac{1}{\hbar^2}\sum_k \int_{t_0}^{t} dt' {\rm Re}[\{V_{ki}(R(t), P(t)), V_{ik}(R(t'), P(t')) \\ &\quad \times [n_k(t') - n_i(t')]\}_+ e^{i\omega_{ik}(t-t')}]. \end{aligned} \tag{8}$$

Here, $\{G_1, G_2\}_+ = G_1G_2 + G_2G_1$ and t_0 is starting time of the process. Following the random-phase approximation, the term $2/\hbar\sum_k {\rm Im}\{V_{ki}(R(t), P(t))n_{ki}(t_0)e^{i\omega_{ik}(t-t_0)}\}$ is disregarded in Eq. (8). Equation (8) resembles in its structure a master equation, but, in contrast to this equation, it takes into consideration the memory effects due to its integral nature. The process of intense excitation of the nuclei affects a large number of single-particle states. Therefore, the occupation number $n_i(t)$ of each level changes very slowly with time. In addition, the kernel of the integro-differential Eq. (8) has a sharp maximum at $t = t'$.

The system of Heisenberg equations of motion for the collective variables R and P is obtained by commuting them with H:

$$\begin{aligned} \frac{d}{dt}R(t) &= \frac{i}{\hbar}[H, R(t)] = \frac{P(t)}{\mu} + \sum_{ik}\frac{\partial V_{ik}(R(t), P(t))}{\partial P(t)}n_{ik}(t), \\ \frac{d}{dt}P(t) &= \frac{i}{\hbar}[H, P(t)] = -\frac{\partial U(R(t))}{\partial R(t)} \\ &\quad - \sum_{ik}\frac{\partial V_{ik}(R(t), P(t))}{\partial R(t)}n_{ik}(t). \end{aligned} \tag{9}$$

If we substitute Eq. (7) into Eqs. (9), we obtain a set of nonlinear integro-differential stochastic dissipative equations

$$\begin{aligned} \frac{d}{dt}R(t) &= \frac{P(t)}{\tilde{\mu}} + \frac{1}{2}\int_{t_0}^{t} dt' \{K_{PR}(t, t'), \dot{R}(t')\}_+ \\ &\quad + \frac{1}{2}\int_{t_0}^{t} dt' \{K_{PP}(t, t'), \dot{P}(t')\}_+ + F_R(t), \\ \frac{d}{dt}P(t) &= -\frac{\partial\tilde{U}(R(t))}{\partial R(t)} - \frac{1}{2}\int_{t_0}^{t} dt' \{K_{RR}(t, t'), \dot{R}(t')\}_+ \\ &\quad - \frac{1}{2}\int_{t_0}^{t} dt' \{K_{RP}(t, t'), \dot{P}(t')\}_+ - F_P(t). \end{aligned} \tag{10}$$

Here,

$$\frac{P(t)}{\tilde{\mu}} = \frac{P(t)}{\mu} - \frac{1}{2}\sum_{ik}\frac{n_k(t) - n_i(t)}{\hbar\omega_{ik}}\frac{\partial|V_{ik}(R(t), P(t))|^2}{\partial P(t)}$$

and

$$\tilde{U}(R(t)) = U(R(t)) - \frac{1}{2}\sum_{ik}\frac{n_k(t) - n_i(t)}{\hbar\omega_{ik}}|V_{ik}(R(t), P(t))|^2,$$

where $\tilde{\mu}$ and $\tilde{U}$ are the renormalized reduced mass parameter and potential energy, respectively. The dissipative kernels in Eqs. (10) are:

$$\begin{aligned} K_{PR}(t, t') &= \sum_{ik}\frac{1}{2\hbar\omega_{ik}} \\ &\quad \times {\rm Re}\left[\left\{\frac{\partial V_{ik}(R(t), P(t))}{\partial P(t)}, \frac{\partial V_{ki}(R(t'), P(t'))}{\partial R(t')}\right. \right. \\ &\quad \left.\left. \times [n_k(t') - n_i(t')]\right\}_+ e^{i\omega_{ki}(t-t')}\right], \end{aligned}$$

$$K_{PP}(t,t') = \sum_{ik} \frac{1}{2\hbar\omega_{ik}} \times \mathrm{Re}\left[\left\{\frac{\partial V_{ik}(R(t),P(t))}{\partial P(t)}, \frac{\partial V_{ki}(R(t'),P(t'))}{\partial P(t')} \times [n_k(t') - n_i(t')]\right\}_+ e^{i\omega_{ki}(t-t')}\right],$$
$$K_{RP}(t,t') = \sum_{ik} \frac{1}{2\hbar\omega_{ik}} \times \mathrm{Re}\left[\left\{\frac{\partial V_{ik}(R(t),P(t))}{\partial R(t)}, \frac{\partial V_{ki}(R(t'),P(t'))}{\partial P(t')} \times [n_k(t') - n_i(t')]\right\}_+ e^{i\omega_{ki}(t-t')}\right],$$
$$K_{RR}(t,t') = \sum_{ik} \frac{1}{2\hbar\omega_{ik}} \times \mathrm{Re}\left[\left\{\frac{\partial V_{ik}(R(t),P(t))}{\partial R(t)}, \frac{\partial V_{ki}(R(t'),P(t'))}{\partial R(t')} \times [n_k(t') - n_i(t')]\right\}_+ e^{i\omega_{ki}(t-t')}\right]. \quad (11)$$

These kernels contain the occupation numbers and, thus, are dependent on the temperature. The fluctuations enter in the analysis through the specification of the distribution of the initial conditions. In Eqs. (10) the operators of random forces in the coordinate and momentum are

$$F_R(t) = \sum_{ik} \frac{\partial V_{ik}(R(t),P(t))}{\partial P(t)} n_{ik}(t_0) e^{i\omega_{ki}(t-t_0)} = \sum_{ik} F_R^{ik}(t) \quad (12)$$

and

$$F_P(t) = \sum_{ik} \frac{\partial V_{ik}(R(t),P(t))}{\partial R(t)} n_{ik}(t_0) e^{i\omega_{ki}(t-t_0)} = \sum_{ik} F_P^{ik}(t), \quad (13)$$

respectively. Following the usual procedure of statistical mechanics, we identify the operators $F_R^{ik}(t)$ and $F_P^{ik}(t)$ as fluctuations because of the uncertainty in the initial conditions for the operators of the internal subsystem [14,29,30]. The statistical properties of random forces are

$$\langle\langle n_{ik}(t)\rangle\rangle = \langle\langle F_P^{ik}(t)\rangle\rangle = \langle\langle F_R^{ik}(t)\rangle\rangle = \langle\langle F_P(t)\rangle\rangle = \langle\langle F_R(t)\rangle\rangle = 0, \quad (14)$$

$$\langle\langle F_R(t)F_R(t')\rangle\rangle \neq 0, \quad \langle\langle F_R(t)F_P(t')\rangle\rangle \neq 0, \quad \langle\langle F_P(t)F_P(t')\rangle\rangle \neq 0, \quad \langle\langle F_P(t)F_R(t')\rangle\rangle \neq 0, \quad \langle\langle n_{ik}(t_0)n_{k'i'}(t_0)\rangle\rangle = \delta_{ik'}\delta_{ki'}\bar{n}_i(t_0)[1-\bar{n}_k(t_0)], \quad (15)$$

where $\bar{n}_i = \langle\langle n_i\rangle\rangle$. The symbol $\langle\langle ...\rangle\rangle$ denotes the average over the intrinsic degrees of freedom. There are the fluctuation-dissipation relations between the dissipation of the collective subsystem and the fluctuations $\varphi_{nm}^{ik}(t,t') = \frac{1}{2}\langle\langle F_n^{ik}(t)F_m^{ki}(t') + F_m^{ki}(t')F_n^{ik}(t) + F_n^{ik}(t')F_m^{ki}(t) + F_m^{ki}(t)F_n^{ik}(t')\rangle\rangle$ $(n,m = R,P)$ of random forces:

$$\sum_{ik}\varphi_{RR}^{ik}(t,t')\frac{1}{\hbar\omega_{ik}}\frac{\bar{n}_k(t') - \bar{n}_i(t')}{\bar{n}_i(t_0)[1-\bar{n}_k(t_0)] + \bar{n}_k(t_0)[1-\bar{n}_i(t_0)]} = \langle\langle K_{RR}(t,t')\rangle\rangle,$$
$$\sum_{ik}\varphi_{PP}^{ik}(t,t')\frac{1}{\hbar\omega_{ik}}\frac{\bar{n}_k(t') - \bar{n}_i(t')}{\bar{n}_i(t_0)[1-\bar{n}_k(t_0)] + \bar{n}_k(t_0)[1-\bar{n}_i(t_0)]} = \langle\langle K_{PP}(t,t')\rangle\rangle,$$
$$\sum_{ik}\varphi_{PR}^{ik}(t,t')\frac{1}{\hbar\omega_{ik}}\frac{\bar{n}_k(t') - \bar{n}_i(t')}{\bar{n}_i(t_0)[1-\bar{n}_k(t_0)] + \bar{n}_k(t_0)[1-\bar{n}_i(t_0)]} = \langle\langle K_{PR}(t,t')\rangle\rangle,$$
$$\sum_{ik}\varphi_{RP}^{ik}(t,t')\frac{1}{\hbar\omega_{ik}}\frac{\bar{n}_k(t') - \bar{n}_i(t')}{\bar{n}_i(t_0)[1-\bar{n}_k(t_0)] + \bar{n}_k(t_0)[1-\bar{n}_i(t_0)]} = \langle\langle K_{RP}(t,t')\rangle\rangle. \quad (16)$$

We assume that the collective motion is sufficiently slow and the intrinsic degrees of freedom are close to those of local equilibrium for each value of the collective variable. Approximating the occupation numbers in terms of Fermi-Dirac occupation factors $\bar{n}_i = \exp[(\varepsilon_i - \varepsilon_F)/T + 1]^{-1}$ (ε_F is the energy of Fermi), we express the fluctuation-dissipation relations as (16) but with the replacements

$$\frac{\bar{n}_k(t') - \bar{n}_i(t')}{\bar{n}_i(t_0)[1-\bar{n}_k(t_0)] + \bar{n}_k(t_0)[1-\bar{n}_i(t_0)]} \to \tanh\left(\frac{\hbar\omega_{ik}}{2T}\right).$$

These relations, which combine the thermal and quantal fluctuations, are valid at all temperatures. The quantum fluctuation-dissipation relations differ from the classical ones and are reduced to them in the limit of high temperature (or $\hbar \to 0$). The effective temperature converges to the thermodynamical temperature when the thermal energy dominates with respect to the average zero-point motion energy of internal subsystem: $\overline{\hbar\omega_{ik}} \ll 2T$. The validity of Eqs. (16) means that we have properly identified the dissipative and fluctuating terms in the non-Markovian dynamical equations of motion.

B. Derivation of equations for first and second moments

Approximating locally the renormalized potential by a harmonic or an inverted oscillator, $\tilde{U} = \delta R^2/2$, assuming that in Eqs. (10) the functionals $\tilde{\mu}, \partial V_{ik}(R(t),P(t))/\partial P(t)$ and $\partial V_{ik}(R(t),P(t))/\partial R(t)$ weakly dependent on fluctuations of P and R in the considered interval of $t - t_0 \to t$, and replacing P and R in these functionals by their average values, we obtain the set of generalized non-Markovian equations which can be solved analytically [14]. Applying the Laplace transformation $\mathcal{L}$ to Eqs. (10), we obtain the set of linear equations for the transforms. For the solution of this system of equations, one should find the roots s_i of its determinant

$$d(s) = s^2[1 + K_{PR}(s)][1 - K_{RP}(s)] + [\tilde{\delta} + sK_{RR}(s)] \times [1/\tilde{\mu} + sK_{PP}(s)].$$

The explicit solutions are

$$R(t) = A_t R(0) + B_t P(0) + \int_0^t d\tau [C_\tau F_R(t-\tau) + \tilde{C}_\tau F_P(t-\tau)],$$

$$P(t) = M_t R(0) + N_t P(0) + \int_0^t d\tau [L_\tau F_P(t-\tau) + \tilde{L}_\tau F_R(t-\tau)], \quad (17)$$

where the time-dependent coefficients are denoted as follows:

$$A_t = \mathcal{L}^{-1}\left\{\frac{s[1+K_{PR}(s)][1-K_{RP}(s)] + [1/\tilde{\mu} + sK_{PP}(s)]K_{RR}(s)}{d(s)}\right\},$$
$$N_t = \mathcal{L}^{-1}\left\{\frac{s[1-K_{RP}(s)][1+K_{PR}(s)] + [\tilde{\delta} + sK_{RR}(s)]K_{PP}(s)}{d(s)}\right\}, \quad B_t = \mathcal{L}^{-1}\left\{\frac{\tilde{\mu}^{-1}[1-K_{RP}(s)]}{d(s)}\right\},$$
$$M_t = -\mathcal{L}^{-1}\left\{\frac{\tilde{\delta}[1+K_{PR}(s)]}{d(s)}\right\}, \quad C_t = \mathcal{L}^{-1}\left\{\frac{s[1-K_{RP}(s)]}{d(s)}\right\}, \quad L_t = \mathcal{L}^{-1}\left\{\frac{s[1+K_{PR}(s)]}{d(s)}\right\},$$
$$\tilde{C}_t = \mathcal{L}^{-1}\left[\frac{1/\tilde{\mu} + sK_{PP}(s)}{d(s)}\right], \quad \tilde{L}_t = -\mathcal{L}^{-1}\left[\frac{\tilde{\delta} + sK_{RR}(s)}{d(s)}\right].$$

Here, $\mathcal{L}^{-1}$ means the inverse Laplace transformation and $K_{RR}(s)$, $K_{PP}(s)$, $K_{PR}(s)$, $K_{RP}(s)$ are the Laplace transforms of the dissipative kernels. The subscripts t and τ denote the time dependence. The exact solutions $R(t)$ and $P(t)$ in terms of roots s_i can be given by the residue theorem [14].

To determine the friction and diffusion coefficients, we consider the equations for the first moment and the variances in the coordinate $\sigma_{RR}(t) = \langle R^2(t)\rangle - \langle R(t)\rangle^2$ and in the momentum $\sigma_{PP}(t) = \langle P^2(t)\rangle - \langle P(t)\rangle^2$ and for the mixed variance $\sigma_{PR}(t) = \frac{1}{2}\langle P(t)R(t) + R(t)P(t)\rangle - \langle P(t)\rangle\langle R(t)\rangle$. Making derivative of Eqs. (17) in t and simple but tedious algebra, we obtain the following equations [14]:

$$\begin{aligned}
\langle \dot{R}(t)\rangle &= -\lambda_R(t)\langle R(t)\rangle + \frac{1}{m(t)}\langle P(t)\rangle,\\
\langle \dot{P}(t)\rangle &= -\xi(t)\langle R(t)\rangle - \lambda_P(t)\langle P(t)\rangle,\\
\dot{\sigma}_{RR}(t) &= -2\lambda_R(t)\sigma_{RR}(t) + \frac{2}{m(t)}\sigma_{PR}(t) + 2D_{RR}(t),\\
\dot{\sigma}_{PP}(t) &= -2\lambda_P(t)\sigma_{PP}(t) - 2\xi(t)\sigma_{PR}(t) + 2D_{PP}(t),\\
\dot{\sigma}_{PR}(t) &= -[\lambda_P(t) + \lambda_R(t)]\sigma_{PR}(t) - \xi(t)\sigma_{RR}(t)\\
&\quad + \frac{1}{m(t)}\sigma_{PP}(t) + 2D_{PR}(t).
\end{aligned} \quad (18)$$

The same equations were derived within density matrix formalism in Refs. [18,24] where the approximate expressions for transport coefficients are obtained. From the structure of Eqs. (18) it is seen that the dynamics of system is ruled by the nonstationary friction coefficients in the coordinate $\lambda_R(t)$ and momentum $\lambda_P(t)$, by the mass parameter $m(t)$, by the stiffness coefficient $\xi(t)$, by the diffusion coefficients in coordinate $D_{RR}(t)$ and momentum $D_{PP}(t)$, and by the mixed diffusion coefficient in coordinate-momentum $D_{PR}(t)$. These transport coefficients expressed through the time-dependent coefficients of solutions of the equations of motion (17) and the correlators of the random forces are given in Refs. [14]. Thus, we have obtained the Markovian-type (local in time) equations for the first and second moments but with the general form of transport coefficients that explicitly depend on time. The general coupling in the coordinate and momentum gives us nonzero diffusion and friction coefficients in the coordinate and momentum because two random forces $F_R(t)$ and $F_P(t)$ are incorporated in the equations of motion. For the given coupling, the fluctuation-dissipation relations are exactly satisfied in the forms (16). It can be shown that the appropriate canonical equilibrium distribution is achieved in the course of the time evolution of harmonic oscillator.

As shown in Refs. [31], the tunneling through a potential barrier and decay of a metastable state crucially depend on the transport coefficients. The passing of a barrier is larger in the case of $D_{RR} \neq 0$ due to a stronger coherence between different states. For the harmonic oscillator the dissipation rate increases with $\lambda_R(t)$ and $\lambda_P(t)$ but decreases with increasing $D_{PP}(t)$ and $D_{RR}(t)$. For the case of inverted oscillator, $\xi < 0$, the friction in coordinate $\lambda_R(t)$ increases the value of E, but the diffusion coefficient in coordinate $D_{RR}(t)$ decreases it.

III. APPLICATION TO LINEAR COUPLING IN COORDINATE

The dominant contributions to the friction and diffusion coefficients arise from the coupling matrix element V_{ik} over the single-particle energy interval $|\varepsilon_i - \varepsilon_k| \approx \Delta = 6$ MeV (the major shell spacing in the heavy nuclei) which is much larger then the typical value of collective frequency $\hbar\tilde{\omega} = 1$ MeV considered here. If the single-partical spectrum is sufficiently dense, the magnitude of coupling matrix elements $|\partial V_{ik}/\partial R|^2$ and $|\partial V_{ik}/\partial P|^2$ must decrease as a function of energy difference, mainly as a result of the mismatch of the overlap of the wave functions. We can represent this behavior by the Lorentzian function [8,24,32]

$$|\partial V_{ik}/\partial R|^2, |\partial V_{ik}/\partial P|^2 \sim \frac{1}{\pi}\frac{\hbar^2\gamma^2}{\hbar^2\gamma^2 + (\varepsilon_i - \varepsilon_k)^2},$$

where $\hbar\gamma = 2\Delta$. One can replace the energy difference $|\varepsilon_i - \varepsilon_k|$ with $\hbar\omega_0$ and approximately take the Lorentzian for the frequency ω_0, and convert the summation over the single-particle states to the integral in frequency:

$$\begin{aligned}\sum_{ik} \frac{|\partial V_{ik}/\partial R|^2(\overline{n}_k - \overline{n}_i)}{\hbar^2\omega_{ik}}\ldots &= \int_0^\infty d\omega_0 \sum_{ik} \delta(\omega_0 - \omega_{ik}) \frac{|\partial V_{ik}/\partial R|^2(\overline{n}_k - \overline{n}_i)}{\hbar^2\omega_{ik}}\ldots \\ &\approx \frac{\tilde{\lambda}}{\pi}\int_0^\infty d\omega_0 \frac{\gamma^2}{\gamma^2+\omega_0^2}\ldots,\end{aligned}$$

where $\tilde{\lambda}$ is related to the strength of coupling between collective and internal subsystems, and $g(\omega_0) = \sum_{ik}\delta(\omega_0 - \omega_{ik}) \sim \omega_0$ is the level density [27].

For a damped quantum oscillator $\tilde{U}(R) = \pm\mu\omega^2R^2/2 = \delta R^2/2$ (a positive sign stands for a parabolic potential well and a negative sign for a parabolic potential barrier) with linear coupling in coordinate R ($\partial V_{ij}/\partial P = 0$, $\partial V_{ij}/\partial R \neq 0$), the expressions for transport coefficients in Eqs. (18) are [14]

$$\begin{aligned}\lambda_R(t) &= D_{RR}(t) = 0, \quad m(t) = \mu, \\ \lambda_P(t) &= \frac{d}{dt}\ln(B_tM_t - A_tN_t),\end{aligned} \tag{19}$$

$$\xi(t) = \frac{\dot{M}_tN_t - \dot{N}_tM_t}{B_tM_t - A_tN_t}, \tag{20}$$

$$D_{PP}(t) = \lambda_P(t)J_{P_tP_t} + \frac{1}{2}[\dot{J}_{P_tP_t} + \mu\xi(t)\dot{J}_{R_tR_t}], \tag{21}$$

$$D_{PR}(t) = \frac{1}{2}\left\{\xi(t)J_{R_tR_t} - \frac{1}{\mu}J_{P_tP_t} + \frac{\mu}{2}[\lambda_P(t)\dot{J}_{R_tR_t} + \ddot{J}_{R_tR_t}]\right\}, \tag{22}$$

where

$$\begin{aligned}J_{R_tR_t} &= \frac{\hbar^2\tilde{\lambda}\gamma^2}{\pi}\int_0^t d\tau' B_{\tau'}\int_0^t d\tau'' B_{\tau''} \\ &\quad\times\int_0^\infty d\omega\frac{\omega}{\omega^2+\gamma^2}\coth\left[\frac{\hbar\omega}{2T}\right] \\ &\quad\times\cos[\omega(\tau'-\tau'')], \\ J_{P_tP_t} &= \frac{\hbar^2\tilde{\lambda}\gamma^2}{\pi}\int_0^t d\tau' N_{\tau'}\int_0^t d\tau'' N_{\tau''} \\ &\quad\times\int_0^\infty d\omega\frac{\omega}{\omega^2+\gamma^2}\coth\left[\frac{\hbar\omega}{2T}\right] \\ &\quad\times\cos[\omega(\tau'-\tau'')], \\ J_{R_tP_t} + J_{P_tR_t} &= \frac{2\hbar^2\tilde{\lambda}\gamma^2}{\pi}\int_0^t d\tau' N_{\tau'}\int_0^t d\tau'' B_{\tau''} \\ &\quad\times\int_0^\infty d\omega\frac{\omega}{\omega^2+\gamma^2}\coth\left[\frac{\hbar\omega}{2T}\right] \\ &\quad\times\cos[\omega(\tau'-\tau'')],\end{aligned} \tag{23}$$

$$B_t = \frac{1}{\mu}\sum_{i=1}^3 \beta_i(s_i+\gamma)e^{s_it}, \quad N_t = \mu\dot{B}_t, \quad M_t = -\mu\delta B_t,$$

$$A_t = \sum_{i=1}^3 \beta_i[s_i(s_i+\gamma) + \hbar\tilde{\lambda}\gamma/\mu]e^{s_it}.$$

Here, dot means the time derivative, $\beta_1 = [(s_1 - s_2)\times(s_1 - s_3)]^{-1}$, $\beta_2 = [(s_2 - s_1)(s_2 - s_3)]^{-1}$ and $\beta_3 = [(s_3 - s_1)(s_3 - s_2)]^{-1}$, and s_i are the roots of the following equation:

$$d(s) = [(s+\gamma)(s^2 + \delta/\mu) + \hbar\tilde{\lambda}\gamma s/\mu]/(s+\gamma) = 0. \tag{24}$$

For the case of coupling in coordinate between the collective and internal subsystems, the equations for the first and second moments do not contain the terms $\lambda_R(t)$ and $D_{RR}(t)$. This is consequence of the absence of random force $F_R(t)$.

Note that in numerical calculations of the time-dependent transport coefficients all three roots s_i of the cubic Equation (24) are taken into consideration. For the inverted oscillator, the three roots are real: one positive and two negative. For example, for $\hbar(|\xi(\infty)|/\mu)^{1/2} = 1$ MeV we obtain $\hbar s_1 = 0.62, 0.41, 0.30$ MeV, $\hbar s_2 = -1.62, -2.41, -3.30$ MeV, and $\hbar s_3 = -11$, -10, -9 MeV at $\hbar\lambda_P(\infty) = 1$, 2, 3 MeV, respectively. For the harmonic oscillator, the one root is real and negative and two other roots are complex conjugate at $2[\xi(\infty)/\mu]^{1/2} > \lambda_P(\infty)$, and all roots are real and negative at $2[\xi(\infty)/\mu]^{1/2} \leqslant \lambda_P(\infty)$. For example, for $\hbar[\xi(\infty)/\mu]^{1/2} = 1$ MeV we get $\hbar s_1 = -0.50 + i0.87$, -1.0, -0.38 MeV, $\hbar s_2 = -0.50 - i0.87$, -1.0, -2.62 MeV, and $\hbar s_3 = -11$, -10, -9 MeV at $\hbar\lambda_P(\infty) = 1$, 2, 3 MeV, respectively. Note that the values of $\xi(\infty)$ and $\lambda_P(\infty)$ depend on $\tilde{\lambda}$. Below the low indexes are ascribed to the roots in accordance with the following rule: $\mathrm{Re}(s_3) < \mathrm{Re}(s_2) \leqslant \mathrm{Re}(s_1)$, $\mathrm{Im}(s_1) \geqslant 0$.

In accordance with Eqs. (19)–(23) the friction and diffusion coefficients for a parabolic potential well and a parabolic potential barrier have the following form at $t \to \infty$:

$$\begin{aligned}\lambda_P(\infty) &= -(s_2 + s_1), \\ \xi(\infty) &= \delta\frac{(s_1+\gamma)(s_2+\gamma)}{(s_1+\gamma)(s_2+\gamma) - \hbar\tilde{\lambda}\gamma/\mu}, \\ D_{PP}(\infty) &= \lambda_P(\infty)J_{P_\infty P_\infty} + \xi(\infty)\frac{J_{R_\infty P_\infty} + J_{P_\infty R_\infty}}{2}, \\ D_{PR}(\infty) &= \frac{1}{2}\left[\lambda_P(\infty)\frac{J_{R_\infty P_\infty} + J_{P_\infty R_\infty}}{2} + \xi(\infty)J_{R_\infty R_\infty} - \frac{1}{\mu}J_{P_\infty P_\infty}\right],\end{aligned} \tag{25}$$

where

$$\begin{aligned}J_{R_\infty R_\infty} &= \frac{\hbar^2\tilde{\lambda}\gamma^2}{\pi\mu^2}\sum_{i,j}\beta_i\beta_j(s_i+\gamma)(s_j+\gamma)\phi^a(s_i,s_j), \\ J_{P_\infty P_\infty} &= \frac{\hbar^2\tilde{\lambda}\gamma^2}{\pi}\sum_{i,j}\beta_i\beta_j s_i s_j(s_i+\gamma)(s_j+\gamma) \\ &\quad\times\phi^a(s_i,s_j), \\ J_{R_\infty P_\infty} + J_{P_\infty R_\infty} &= \frac{\hbar^2\tilde{\lambda}\gamma^2}{\pi\mu}\sum_{i,j}\beta_i\beta_j(s_i+s_j)(s_i+\gamma) \\ &\quad\times(s_j+\gamma)\phi^a(s_i,s_j),\end{aligned}$$

$$\phi^a(s_i, s_j) = \frac{s_j\psi[-\hbar s_j/(2\pi T)]}{(s_i+s_j)(s_j^2-\gamma^2)} + \frac{s_i\psi[-\hbar s_i/(2\pi T)]}{(s_i+s_j)(s_i^2-\gamma^2)} + \frac{(\gamma^2 - s_i s_j)\psi[\hbar\gamma/(2\pi T)]}{(\gamma^2-s_i^2)(\gamma^2-s_j^2)} - \frac{\pi T(s_i+s_j-2\gamma)}{\hbar\gamma(s_i+s_j)(\gamma-s_i)(\gamma-s_j)}. \quad (26)$$

The two roots $s_{1,2}$ with $\mathrm{Re}(s_1) > \mathrm{Re}(s_3)$ and $\mathrm{Re}(s_2) > \mathrm{Re}(s_3)$ are taken in $\lambda_P(\infty)$ and $\xi(\infty)$. There is no contribution of the third root s_3 of Eq. (24) into $\lambda_P(\infty)$ and $\xi(\infty)$. In the Eq. (26) all three roots are presented. In expressions (26) $\psi(z) = \Gamma'(z)/\Gamma(z)$, where $\Gamma(z)$ is a γ function and $\Gamma'(z) = d\Gamma(z)/dz$. Thus, in quantum treatment there are two diffusion coefficients D_{PP} and D_{PR} instead of one diffusion coefficient $D_{PP} = D^c_{PP}$ in the classical limit.

In the case of parabolic potential well the expressions for the $J_{n_\infty m_\infty}$ are simplified:

$$J_{R_\infty R_\infty} = \frac{\hbar^2\tilde{\lambda}\gamma^2}{\pi\mu^2}\int_0^\infty d\omega_0 \frac{\omega_0 \coth[\hbar\omega_0/(2T)]}{(s_1^2+\omega_0^2)(s_2^2+\omega_0^2)(s_3^2+\omega_0^2)},$$
$$J_{P_\infty P_\infty} = \frac{\hbar^2\tilde{\lambda}\gamma^2}{\pi}\int_0^\infty d\omega_0 \frac{\omega_0^3 \coth[\hbar\omega_0/(2T)]}{(s_1^2+\omega_0^2)(s_2^2+\omega_0^2)(s_3^2+\omega_0^2)},$$
$$J_{R_\infty P_\infty} + J_{P_\infty R_\infty} = 0. \quad (27)$$

IV. ILLUSTRATIVE CALCULATIONS FOR HARMONIC AND INVERTED OSCILLATORS

A. Diffusion coefficients

To illustrate the influence of the quantum effects on the dynamics of the initial stage of reaction at energies near the Coulomb barrier, we consider, as an example, the evolution of the system ^{100}Mo+^{100}Mo in the relative distance R. Note that the results obtained would be qualitatively universal for other reactions. During the approach stage of collision, the system overcomes the Coulomb barrier, the main part of the initial kinetic energy is dissipated into the internal excitations, and the touching configuration is formed. The dependence of the potential energy of this system on the coordinate R is approximated by the inverted oscillator with frequency $\hbar\tilde{\omega} =$ 1 MeV. The reduced mass parameter is $\mu = 50m_0$ (where m_0 is the nucleon mass). The diffusion and friction coefficients depend on the parameters ω, $\tilde{\lambda}$, and γ. We set $\hbar\gamma = 12$ MeV. The value of γ holds the condition $\gamma \gg \tilde{\omega}$ [14,29]. The dependence of diffusion coefficients on γ is rather weak. The values of ω and $\tilde{\lambda}$ are fixed by given certain asymptotic values of $\xi(\infty)$ and $\lambda_P(\infty)$

$$\xi(\infty) = \xi = \tilde{\delta} = \mu\tilde{\omega}^2, \quad \lambda_P(\infty) = \lambda_P.$$

Near the Coulomb barrier the used values $\hbar\lambda_P =$ (1–3) MeV are consistent with those extracted from the experimental data on the heavy-ion reactions [2].

To describe the sub-barrier fusion, the role of transport coefficients in the barrier penetration should be clarified. The time dependencies of the microscopic friction [Eq. (19)] and diffusion [Eqs. (21) and (22)] coefficients are shown in Figs. 1 and 2 for the harmonic and inverted oscillators

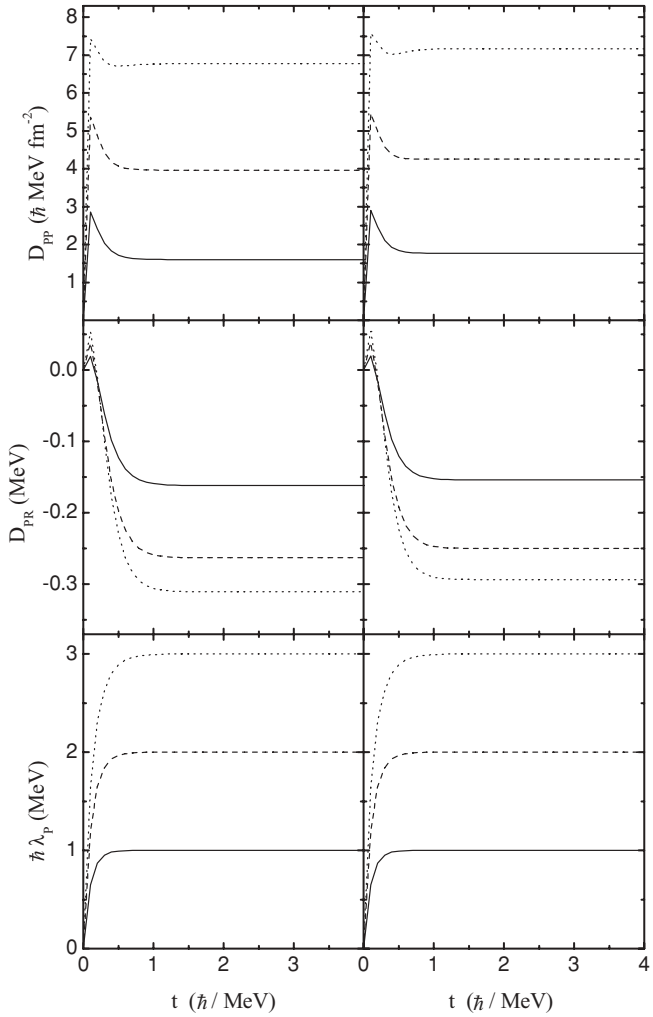

FIG. 1. The calculated time dependence of microscopic diffusion [Eqs. (21) and (22)] and friction [Eq. (19)] coefficients for the inverted (the left-hand side) and harmonic (the right-hand side) oscillators at $T = 1$ MeV. The results leading to the asymptotic friction coefficients $\hbar\lambda_P = 1$, 2, and 3 MeV are presented by solid, dashed, and dotted lines, respectively.

that have the same parameters. All three roots of Eq. (24) are taken into account. The values of D_{PP}, D_{PR}, and λ_P are equal to zero at initial time. In short transient time $\sim\gamma^{-1}$ the coefficients take asymptotic values. The transient time slightly increases with λ_P. During a short initial time interval the value of D_{PR} is positive and becomes negative later on. The mixed diffusion coefficient arises from the non-Markovian character of dynamics. It is absent in the Markovian limit ($\gamma \to \infty$). At high temperature ($T = 1$ MeV) the asymptotic values of diffusion coefficients for the inverted and harmonic oscillators almost coincide with the accuracy about of 6–11% (5%). The deviation increases with decreasing temperature. At low temperature ($T = 0.3$ MeV), the values of $D_{PP}(\infty)$ [$D_{PR}(\infty)$] for the harmonic oscillator ($\hbar\tilde{\omega} = 1$ MeV) are larger of 45% (17%), 20% (13%), and 13% (12%) than those for the inverted oscillator ($\hbar\tilde{\omega} = 1$ MeV) at $\hbar\lambda_P(\infty) =$ 1, 2, and 3 MeV, respectively. For the comparison with the asymptotic values of the microscopical diffusion coefficients

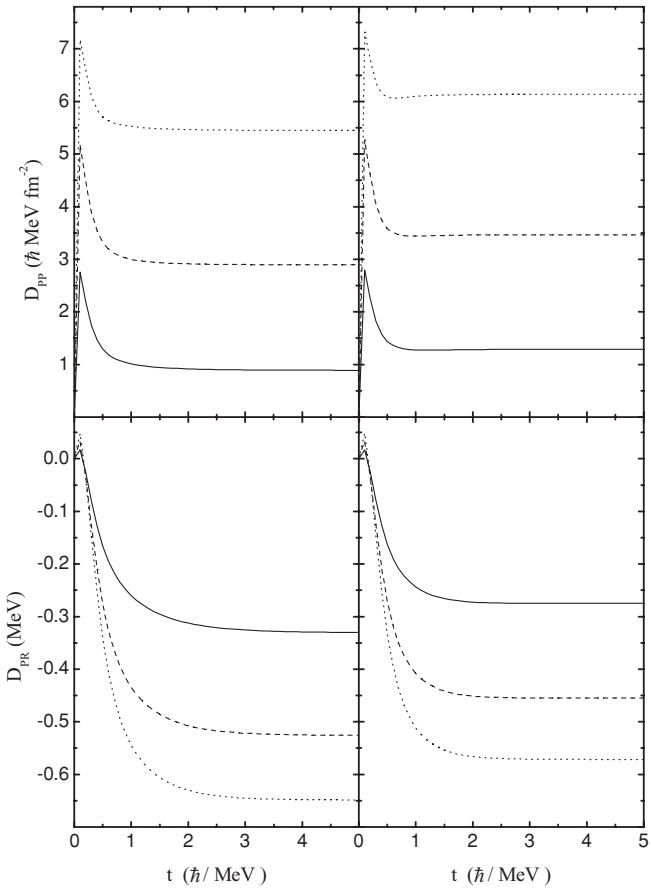

FIG. 2. The same as in Fig. 1, but for $T = 0.3$ MeV.

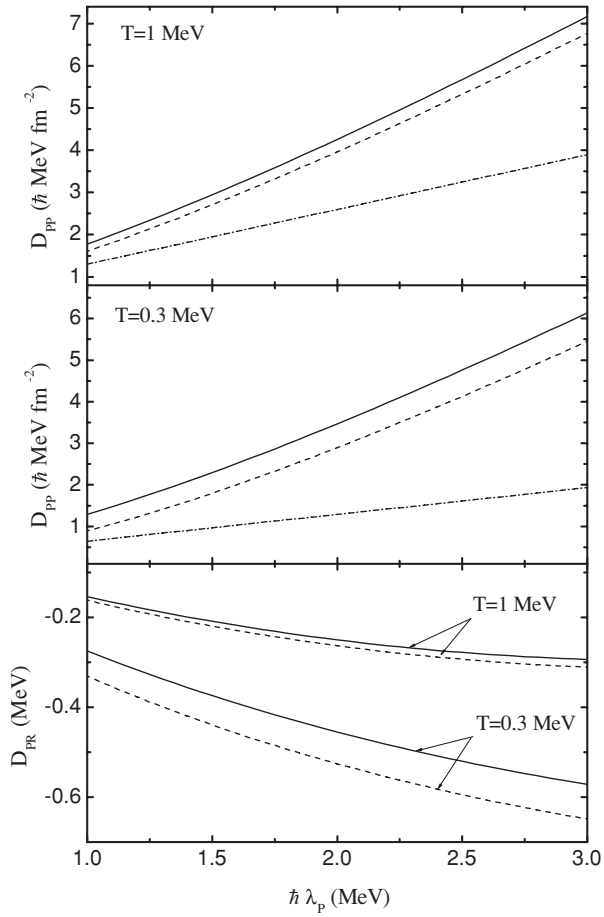

FIG. 3. The calculated asymptotic diffusion coefficients as function of asymptotic friction coefficient for the indicated temperatures. The results for the microscopic diffusion coefficients [Eqs. (21) and (22)] for the harmonic (solid line) and inverted (dashed line) oscillators, and the phenomenological diffusion coefficient [Eq. (28)] in momentum (dash-dotted line) are presented.

$D_{PP}(\infty)$ obtained for the inverted and harmonic oscillators, the dependence of phenomenological diffusion coefficient in momentum

$$D^c_{PP} = \lambda_p \frac{\hbar\tilde{\omega}}{2} \coth\left[\hbar\tilde{\omega}/(2T)\right] \tag{28}$$

on $\lambda_P(\infty)$ is presented at two temperatures in Fig. 3 ($D^c_{PR} = 0$). Note that D^c_{PP} partly contains the quantum effects. In all cases D^c_{PP} is smaller than the microscopically calculated D_{PP}. This difference increases with λ_P but decreases with increasing T. So, the purely microscopic treatment is necessary at the low temperatures and large frictions.

The asymptotic values of $D_{PP}(t)$ and $D_{PR}(t)$ as functions of T are shown in Fig. 4 at $\hbar\lambda_p = 1$ and 3 MeV. D_{PP} depends nearly linear on T at $T \geqslant \hbar\tilde{\omega}/2$. For smaller $\tilde{\omega}$ in Fig. 4, the dependence of D_{PP} on T is rather weak because of the importance of quantum effects. With increasing temperature the absolute value of D_{PR} decreases approaching to zero in the limit of $T \to \infty$.

Figure 5 demonstrates the behavior of the microscopic diffusion coefficients $D_{PP}(\infty)$ and $D_{PR}(\infty)$ (25) at transition from the harmonic oscillator to the inverted oscillator. This transition corresponds to the change of the sign of stiffness coefficient ξ. The asymptotic values of $D_{PP}(\infty)$ and $D_{PR}(\infty)$ smoothly change across the point $\tilde{\omega} = 0$. In the considered range of frequencies the absolute values of $D_{PP}(\infty)$ and $D_{PR}(\infty)$ for the inverted and harmonic oscillators are almost close to each other at the finite collective frequency and temperature. The difference of diffusion coefficients for negative and positive stiffness decreases with increasing temperature.

B. Peculiarities for inverted oscillator at low temperature

The results demonstrate that there are limitations in applying the microscopical diffusion coefficients to the inverted oscillator at low temperatures $T \leqslant T_{\rm cr} = \hbar s_1/(2\pi)$, where $T_{\rm cr}$ is the crossover temperature of the transition between thermal activation and quantum tunneling escape, and s_1 is the positive root of Eq. (24). At $T \leqslant T_{\rm cr}$ the values of $D_{PP}(t)$ and $D_{PR}(t)$ have no asymptotics and diverge as functions of time so that diagonal element $D_{PP}(t)$ may become zero or even negative. It is seen in Fig. 4 that the deviations of the values of $D_{PP}(t)$ and $D_{PR}(t)$ from those for the harmonic oscillator grow when T approaches to $T_{\rm cr}$ from above. In the case of inverted oscillator with $\hbar\tilde{\omega} = 1$ MeV we get $T_{\rm cr} = 0.1$ and 0.05 MeV at $\hbar\lambda_P = 1$ and 3 MeV, respectively. Such small

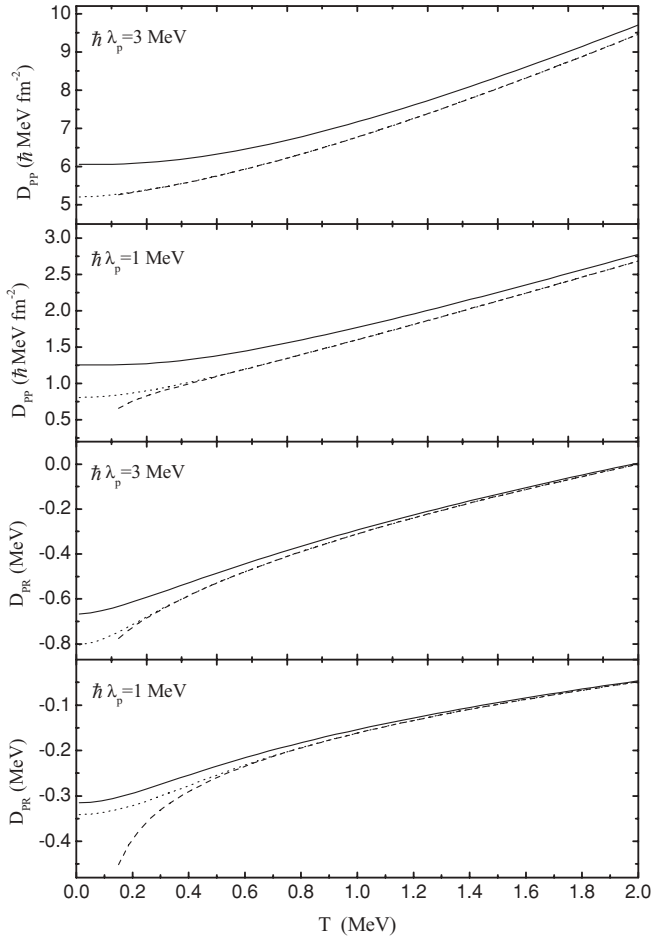

FIG. 4. The calculated asymptotic diffusion coefficients as function of temperature for the indicated asymptotic friction coefficients. The results for the microscopic diffusion coefficients [Eqs. (21) and (22)] for the harmonic (solid line) and inverted (dashed line) oscillators and the modified microscopic diffusion coefficients $D_{PP}(t = 1/s_1)$ and $D_{PR}(t = 1/s_1)$ for the inverted oscillator (dotted line) are presented.

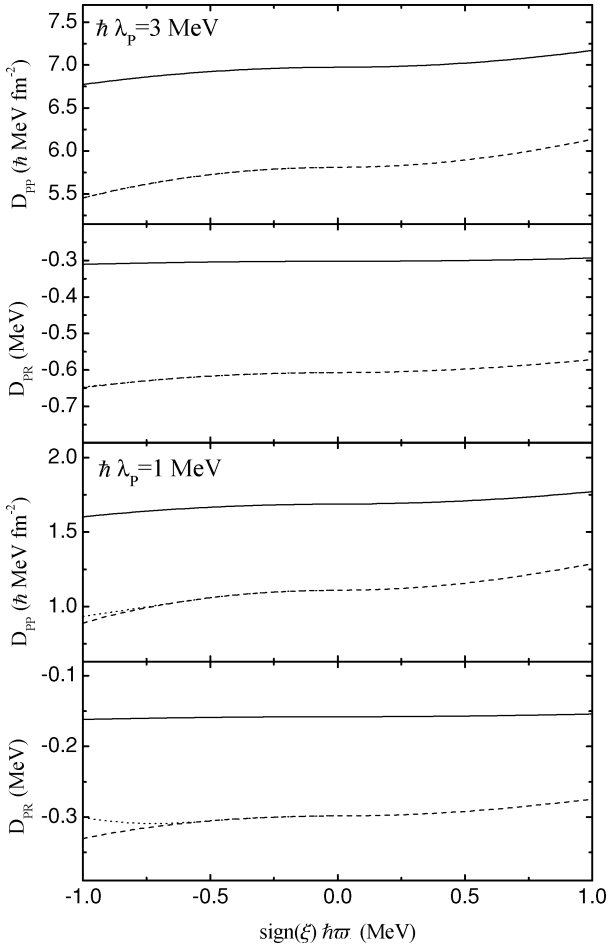

FIG. 5. The calculated asymptotic microscopic diffusion coefficients [Eqs. (21) and (22)] as functions of sign(ξ)$\hbar\tilde{\omega}$ for the indicated asymptotic friction coefficients and temperatures $T = 1$ MeV (solid line) and $T = 0.3$ MeV (dashed line). The results for the modified microscopic diffusion coefficient $D_{PP}(t = 1/s_1)$ and $D_{PR}(t = 1/s_1)$ for the inverted oscillator are presented by dotted line at $T = 0.3$ MeV. At $T = 1$ MeV, the values of $D_{PP}(t = 1/s_1)$ and $D_{PR}(t = 1/s_1)$ coincide with the corresponding microscopic diffusion coefficients.

values of T are rarely realized in the nuclear reactions at energies near the Coulomb barrier. The value of $T_{\rm cr}$ becomes smaller with increasing λ_P or with decreasing $\tilde{\omega}$. The physical meaning of diffusion coefficients is lost below $T_{\rm cr}$. This happens because at low temperatures the correlation time of the fluctuations of the random forces $\tau_{\rm cor} = \hbar/T$ [29] is comparable or even larger than the characteristic time $\tau_{\rm coll} = 2\pi/s_1$ of the collective subsystem. In the Markovian limit, $\tau_{\rm coll} = 2\pi/[\sqrt{\tilde{\omega}^2 + (\lambda_P/2)^2} - \lambda_P/2]$. One can improve the behavior of D_{PP} and D_{PR} at $T \leqslant T_{\rm cr}$ by restricting the upper limits of integrals on τ' and τ'' in Eqs. (23). We make the replacement $t \to 1/s_1$ in Eqs. (23), where $1/s_1$ is the time during which the collective system is closed to the top of the barrier with an infinitesimally small momentum ($\delta p = s_1 \delta q$). With this replacement the values of D_{PP} (D_{PR}) obtained for the inverted and harmonic oscillators are closed to each other at low temperatures (Fig. 4). It should be noted that this modification of the diffusion coefficients does not influence on the values of D_{PP} and D_{PR} at high temperatures ($T > T_{\rm cr}$) because the transition time $1/\gamma$ of reaching the asymptotic is smaller than the time $t = 1/s_1$.

C. Passing probability of barrier

Let us study the capture inside of the Coulomb barrier of the initial Gaussian packet moving toward the barrier at $R = R_b = 0$ from the left-hand side with some kinetic energy. With the initial Gaussian distribution the distribution function remains Gaussian at any time in quadratic potential [14]. The capture probability $P_0(t)$ is defined by the passing probability of potential barrier. Calculating $\langle R(t)\rangle$ and $\sigma_{RR}(t)$ with the sets of friction and diffusion coefficients mentioned above, one can use the time-dependent density matrix

$$\rho(R,t) = \frac{1}{\sqrt{2\pi\sigma_{RR}(t)}} e^{-\frac{(R-\langle R(t)\rangle)^2}{2\sigma_{RR}(t)}}$$

in coordinate representation and find the passing probability $P_0(t)$ of a particle through a barrier

$$P_0(t) = \int_{R_b}^{\infty} dR[\rho(R,t) - \rho(R,t=0)] \Big/ \int_{-\infty}^{R_b} dR\rho(R,0) = \frac{\mathrm{Erf}[\langle R(t)\rangle/\sqrt{2\sigma_{RR}(t)}] - \mathrm{Erf}[\langle R(0)\rangle/\sqrt{2\sigma_{RR}(0)}]}{1 - \mathrm{Erf}[\langle R(0)\rangle/\sqrt{2\sigma_{RR}(0)}]}. \quad (29)$$

Because the initial variance $\sigma_{RR}(0)$ is not zero in the quantum treatment, this expression is slightly different from the expression in Refs. [22–25]. We take the initial variances in accordance with the uncertainty relation and use $\sigma_{RR}(0)\sigma_{PP}(0) = \hbar^2/4$ and $\sigma_{PR}(0) = 0$. When the packet approaches the barrier, the value of $P_0(t)$ increases up to the quasistationary value that defines the part of the initial packet penetrated in the right-hand side. The value of $P_0(t)$ depends on $\langle R(t)\rangle$ and the spreading $\sigma_{RR}(t)$ of the wave packet in the direction of barrier. Due to the friction, the value of P_0 depends on the initial position $\langle R(0)\rangle$ of the packet as well as on the initial kinetic energy $E_{\mathrm{kin}}(0) = [\langle P(0)\rangle^2 + \sigma_{PP}(0)]/(2\mu)$. The final barrier passing probability is given by taking the limit $t \to \infty$ in $P_0(t)$. The ratio $\langle R(\infty)\rangle/\sqrt{2\sigma_{RR}(\infty)}$ approaches a finite limit because

$$\langle R(t)\rangle \to \frac{e^{s_1 t}}{\mu(s_1 - s_2)}\Delta_R = \frac{e^{s_1 t}}{\mu(s_1 - s_2)}[\langle P(0)\rangle - \mu s_2\langle R(0)\rangle], \quad (30)$$

and

$$\sigma_{RR}(t) \to \frac{e^{2s_1 t}}{\mu^2(s_1 - s_2)^2}\Delta_{RR}, \quad (31)$$

where

$$\Delta_{RR} = \mu^2 s_2^2\sigma_{RR}(0) - 2\mu s_2\sigma_{PR}(0) + \sigma_{PP}(0) + 2\mu s_2^2 D_{PR}(\infty)/\tilde{\omega} - s_2 D_{PP}(\infty)/\tilde{\omega}^2$$

(see discussion of the roots of Eq. (24) in Sec. III). In the Markovian limit $s_2 = -(\sqrt{\tilde{\omega}^2 + (\lambda_P/2)^2} + \lambda_P/2) < 0$ and $s_1 = -\tilde{\omega}^2/s_2 > 0$. At $\Delta_R = 0$ the trajectory tends to the top of potential barrier. The trajectory with $\langle R(0)\rangle < 0$ and a positive initial momentum $\langle P(0)\rangle$ always stays on the same side at $\Delta_R < 0$ ($\langle P(0)\rangle < -\mu s_2\langle R(0)\rangle$) but crosses the barrier for the $\Delta_R > 0$ ($\langle P(0)\rangle > -\mu s_2\langle R(0)\rangle$). The asymptotic value of P_0 reaches 1 and vanishes at very large positive and negative values of the ratio $\langle R(\infty)\rangle/\sqrt{2\sigma_{RR}(\infty)}$, respectively. The passing probability of a barrier depends on $D_{PP}(\infty)$ and $D_{PR}(\infty)$, i.e., depends on the dynamical fluctuations.

As found above, the negative value of D_{PR} keeps the probability smaller. To obtain the same probability for the case of $D_{PR} = 0$, we should decrease the diffusion coefficient D_{PP}, i.e., use $\kappa_{\mathrm{cl}} D_{PP}$ ($\kappa_{\mathrm{cl}} < 1$) instead of D_{PP}. Using the equality

$$\sigma_{RR}(D_{PR}(\infty), D_{PP}(\infty)) = \sigma_{RR}(D_{PR} = 0, \kappa_{\mathrm{cl}} D_{PP})$$

and explicit analytical expression for $\sigma_{RR}(t)$, one can find the factor

$$\kappa_{\mathrm{cl}} = 1 - \frac{2\mu s_2 D_{PR}}{D_{PP}}, \quad (32)$$

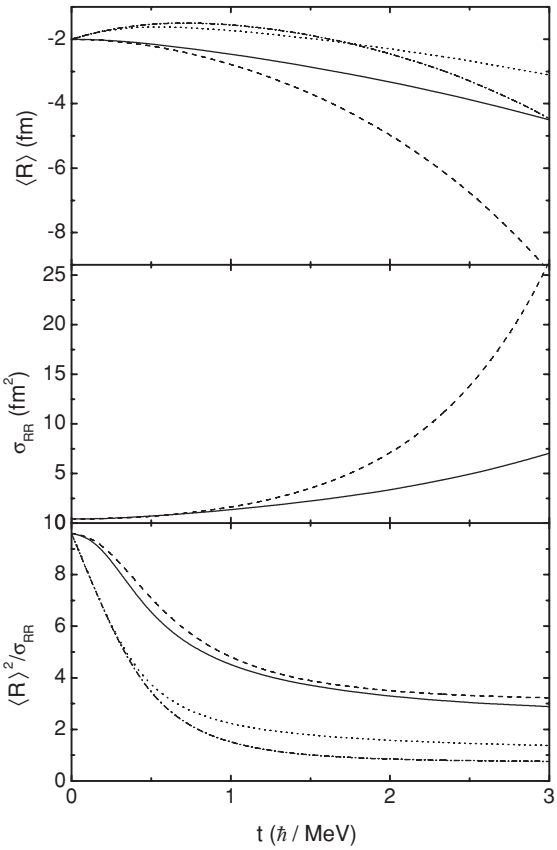

FIG. 6. The calculated dependencies of $\langle R(t)\rangle, \sigma_{RR}(t)$, and $\langle R(t)\rangle^2/\sigma_{RR}(t)$ as functions of time for the relative motion of two nuclei with $\langle R(0)\rangle = -2$ fm, $\sigma_{RR}(0) = 0.42$ fm^2, $\sigma_{PP}(0) = 0.6\hbar^2$ fm^{-2}, $\sigma_{PR}(0) = 0$ in the inverted oscillator potential with $\hbar\tilde{\omega} = 1$ MeV. The results were obtained with the microscopic transport coefficients [Eqs. (19)–(22)] and with $E(0) = -1$ MeV [$\hbar\lambda_P = 1$ MeV (dash-dotted line) and $\hbar\lambda_P = 3$ MeV (dotted line)] and with $E(0) = -2.4$ MeV [$\hbar\lambda_P = 1$ MeV (dashed line) and $\hbar\lambda_P = 3$ MeV (solid line)]. The values of $\sigma_{RR}(t)$ calculated with $E(0) = -1$ and -2.4 MeV coincide.

which gives the effect of D_{PR} on the absolute value of σ_{RR}. If $\kappa_{\mathrm{cl}} \approx 1$, than this effect is weak. The results of calculations show that the role of D_{PR} enhances with decreasing T and λ_P because $\kappa_{\mathrm{cl}} \ll 1$ ($s_2 D_{PR} > 0$).

Figure 6 shows $\langle R(t)\rangle, \sigma_{RR}(t)$, and $\langle R(t)\rangle/\sqrt{2\sigma_{RR}(t)}$ as functions of time for sub-barrier energies at $\hbar\lambda_P = 1$ and 3 MeV. The minimal distance between the center of the wave packet and $R_b = 0$ increases with friction. At the same time, at the distances close to the top of barrier the energy of collective subsystem $E(t)$ at $\hbar\lambda_P = 1$ MeV is larger than one at $\hbar\lambda_P = 3$ MeV (Fig. 7). Therefore, one can expect smaller $\langle R(\infty)\rangle/\sqrt{2\sigma_{RR}(\infty)}$ and, correspondingly, a larger passing probability of a barrier with decreasing λ_P. This effect is clearly demonstrated in Fig. 6 by the behaviors of the dot-dashed and dotted curves for the initial energy $E(0) = -1$ MeV ($\langle P(0)\rangle = 1.9\hbar$ fm^{-1}). However, if the initial energy is small, for example, $E(0) = -2.4$ MeV ($\langle P(0)\rangle = 0$), the passing probability can increase with friction. It can be explained by fact that $E(t)$ at $\hbar\lambda_P = 1$ MeV is smaller than

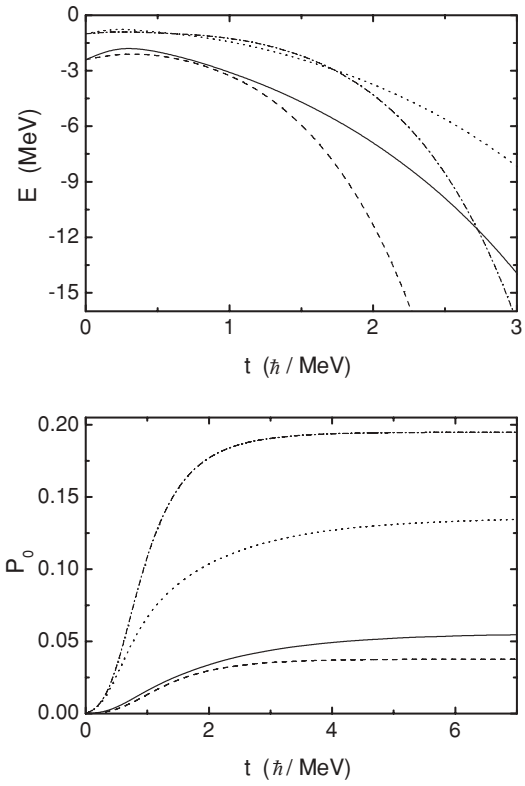

FIG. 7. The calculated dependencies of $E(t)$ and $P_0(t)$ as functions of time for the relative motion of two nuclei with $\langle R(0)\rangle = -2$ fm, $\sigma_{RR}(0) = 0.42$ fm^2, $\sigma_{PP}(0) = 0.6\hbar^2$ fm^{-2}, $\sigma_{PR}(0) = 0$ in an inverted oscillator potential with $\hbar\tilde{\omega} = 1$ MeV. The results were obtained with the microscopic transport coefficients and with $E(0) = -1$ MeV [$\hbar\lambda_P = 1$ MeV (dash-dotted line) and $\hbar\lambda_P = 3$ MeV (dotted line)] and with $E(0) = -2.4$ MeV [$\hbar\lambda_P = 1$ MeV (dashed line) and $\hbar\lambda_P = 3$ MeV (solid line)].

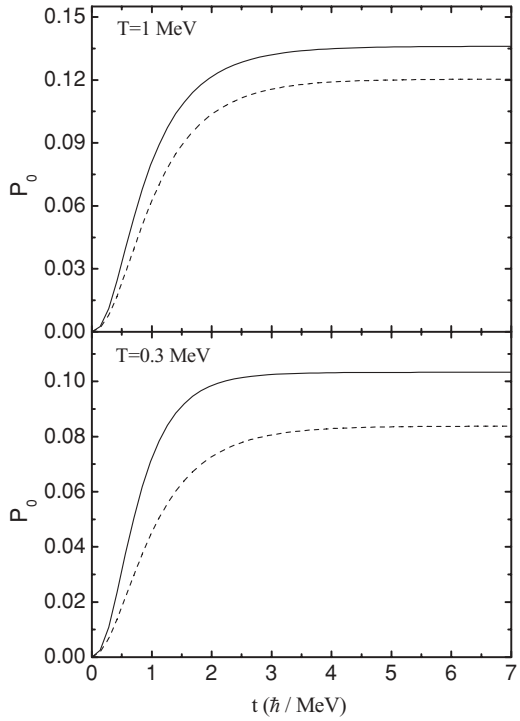

FIG. 8. The calculated probability of capture of the Gaussian packet inside of the barrier (the inverted oscillator potential with $\hbar\tilde{\omega} = 1$ MeV) as function of time for the indicated temperatures at $\langle R(0)\rangle = -1$ fm, $\langle P(0)\rangle = 0$, $\sigma_{RR}(0) = 0.42$ fm^2, $\sigma_{PP}(0) = 0.6\hbar^2$ fm^{-2}, $\sigma_{PR}(0) = 0$, $E(0) = -0.6$ MeV, and $\hbar\lambda_P = 1$ MeV. The results were obtained with the microscopic diffusion coefficients [Eqs. (21) and (22)] (solid line) and with the phenomenological diffusion coefficient [Eq. (28)] in momentum (dashed line).

one at $\hbar\lambda_P = 3$ MeV at the distances close to the top of barrier. At larger friction the dissipation rate of collective subsystem

$$\dot{E}(t) = -2\lambda_P(\infty)E_{\rm kin}(t) + \frac{D_{PP}(\infty)}{\mu} \qquad (33)$$

can be smaller because of smaller kinetic energy and larger diffusion coefficient in momentum. Due to the presence of D_{PP} in Eq. (33) or due to the dynamical fluctuations, one can increase $E(t)$ during short initial time interval (Fig. 7). An increase of the passing probability with friction coefficient or coupling was also found in Refs. [31] when $D_{RR} \neq 0$. An increase of the coupling between the motion in R and internal excitations can be caused by weakly bound neutrons in the projectile and/or target. Thus, some enhancement of the subbarrier fusion can be explained in the reactions with neutron-rich projectiles or targets. In our treatment the neutron transfers are modeled with the values of λ_P and D_{PP}.

Figures 6–8 show the values of $\langle R(t)\rangle/\sqrt{2\sigma_{RR}(t)}$, which reach the asymptotic values in short time about of $2\,\hbar$ MeV^{-1}. Figure 8 demonstrates that with the microscopical set of diffusion coefficients $\{D_{PP}(t), D_{PR}(t)\}$ [Eqs. (21) and (22)] the passing probability is larger than with the phenomenological set $\{D^c_{PP}, D^c_{PR} = 0\}$ [Eq. (28)]. The quantum statistical effects promote the formation of touching nuclear configuration. This is due to the fact that the quantum statistical effects enhance the diffusion. Our capture probabilities are larger than those calculated by the classical formulas in Ref. [25] because of the quantum effects. In spite of $D_{PP}(\infty) > D^c_{PP}$, the difference between $\sigma_{RR}(\infty)$ and $\sigma^c_{RR}(\infty)$, obtained with the microscopical and phenomenological sets of diffusion coefficients, respectively, is quite small due to the negative D_{PR}. It should be noted that the value of $\Delta^{\sigma_{nm}}_{RR} = \mu^2 s_2^2\sigma_{RR}(0) - 2\mu s_2\sigma_{PR}(0) + \sigma_{PP}(0)$ in the expression for Δ_{RR} is comparable or larger than $\Delta^{D_{nm}}_{RR} = 2\mu s_2^2 D_{PR}(\infty)/\tilde{\omega} - s_2 D_{PP}(\infty)/\tilde{\omega}^2$. In the overdamped limit ($\lambda_P > 2\tilde{\omega}$) and at low temperatures ($T \ll 1$ MeV) the value of $P_0(t)$ is insensitive to different sets of the diffusion coefficients because $\Delta^{\sigma_{nm}}_{RR} \gg \Delta^{D_{nm}}_{RR}$. This is more obvious at $2\pi T \ll \hbar\lambda_P$ and $\lambda_P \gg 2\tilde{\omega}$ when we get $\Delta^{D_{nm}}_{RR} \approx 2\mu T\lambda_P^2$.

One can see in Figs. 8–11 that there is no a large deviation of the microscopically calculated asymptotic passing probability $P_0(\infty)$ from $P^c_0(\infty)$ calculated with the phenomenological D^c_{PP} ($D^c_{PR} = 0$). Therefore, the wide use of the phenomenological diffusion coefficients is justified. In the purely quantum regime, $\hbar\omega \gg T$, the value of P^c_0 is smaller than P_0. With increasing T the phenomenological passing probability underestimates the microscopical passing probability. The difference between these passing probabilities

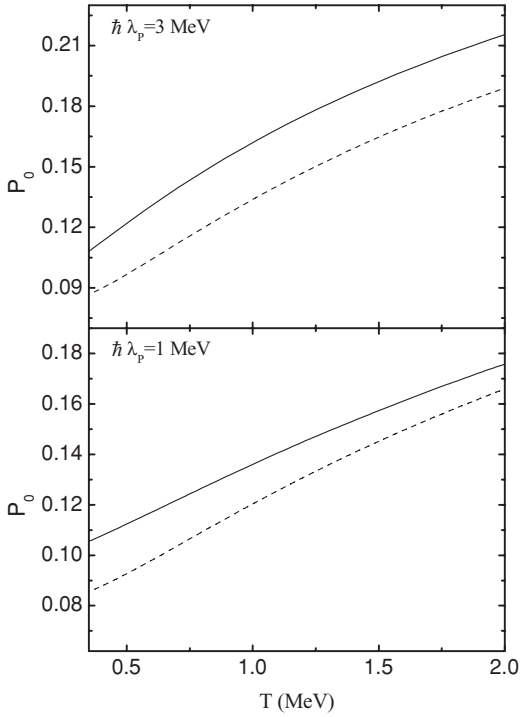

FIG. 9. The calculated asymptotic probability of capture of the Gaussian packet inside of the barrier (the inverted oscillator potential with $\hbar\tilde{\omega} = 1$ MeV) as function of temperature at $\langle R(0)\rangle = -1$ fm, $\langle P(0)\rangle = 0$, $\sigma_{RR}(0) = 0.42$ fm^2, $\sigma_{PP}(0) = 0.6\hbar^2$ fm^{-2}, $\sigma_{PR}(0) = 0$, $E(0) = -0.6$ MeV, and $\hbar\lambda_P = 1$ MeV. The results were obtained with the microscopic diffusion coefficients [Eqs. (21) and (22)] (solid line) and with the phenomenological diffusion coefficient [Eq. (28)] in momentum (dashed line).

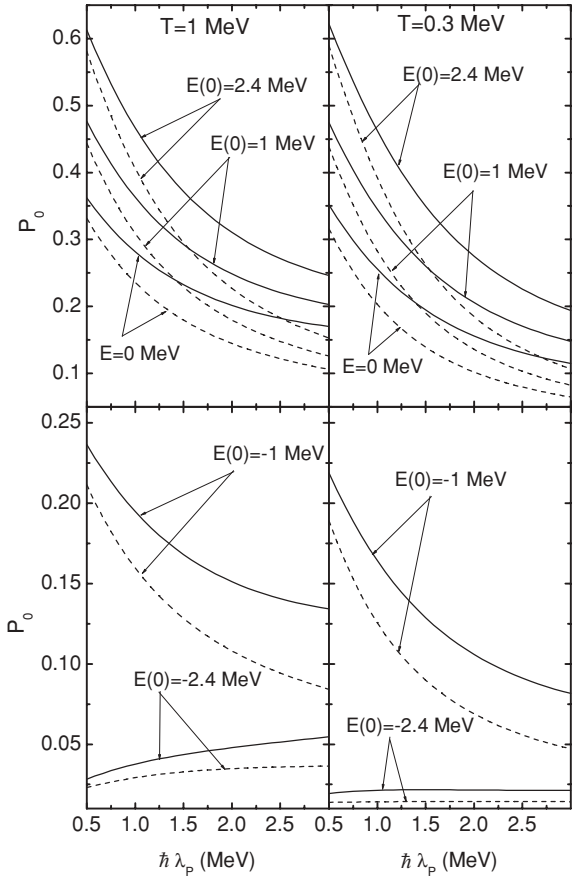

FIG. 10. The calculated asymptotic probability of capture of the Gaussian packet inside of the barrier (the inverted oscillator potential with $\hbar\tilde{\omega} = 1$ MeV) as function of asymptotic friction coefficient for the indicated temperatures and initial energies $E(0)$ at $\langle R(0)\rangle = -2$ fm, $\sigma_{RR}(0) = 0.42$ fm^2, $\sigma_{PP}(0) = 0.6\hbar^2$ fm^{-2}, $\sigma_{PR}(0) = 0$. The results were obtained with the microscopic diffusion coefficients [Eqs. (21) and (22)] (solid line) and with the phenomenological diffusion coefficient [Eq. (28)] in momentum (dashed line).

increases with λ_P. However, the difference between P_0^c and P_0 does not exceed 100% at $\hbar\lambda_P = 3$ MeV. It should be noted that the difference between P_0^c and P_0 increases with mass parameter.

In Fig. 10 the asymptotic values $P_0(\infty)$ as functions of λ_P are shown. The value of P_0 decreases with λ_p at initial energies $E(0) = 2.4$, 1, 0 and -1 MeV. If the initial energy is small, i.e., $E(0) = -2.4$ MeV, the passing probability increases with friction. This is explained by the same way like behavior of P_0 versus λ_P in Fig. 7.

In Fig. 11 the passing probabilities $P_0(t)$ are presented as functions of E or $E_{\rm kin}$. One can see that the role of friction is important in the passing process. Even at energies exceeding the barrier only a part of the packet is penetrated and, thus, $P_0 < 0.5$. The increase of the passing probability with the kinetic energy is slower at $\hbar\lambda_P = 3$ MeV than at $\hbar\lambda_P = 1$ MeV. A deviation of the microscopically calculated asymptotic passing probability P_0 from P_0^c calculated with the phenomenological D_{PP}^c ($D_{PR}^c = 0$) increases with E.

The probability of finding the system on the right-hand side of the barrier varies with the width $\sigma_{RR}(0)$ of the initial wave packet localized to the left of the barrier at $t = 0$ (Fig. 12). This variation is smaller with increasing dissipation and $|\langle R(0)\rangle|$. The value of P_0 reaches the maximum with increasing $\sigma_{RR}(0)$ and decreases later on. Such behavior is because of different rate of change of Erf$[\langle R(\infty)\rangle/\sqrt{2\sigma_{RR}(\infty)}]$ and Erf$[\langle R(0)\rangle/\sqrt{2\sigma_{RR}(0)}]$ for small and large $\sigma_{RR}(0)$. In the considered examples the values of P_0 weakly depends on $\sigma_{RR}(0)$.

V. SUMMARY

Based on the non-Markovian quantum Langevin approach and generalized quantum fluctuation-dissipation relations, the equations of motion with the microscopic transport coefficients explicitly depending on time were derived for the first and second moments in the cases of general coupling and linear coupling in coordinate between the relative motion of interacting nuclei and internal nucleonic degrees of freedom. With the transport coefficients for the damped harmonic and inverted oscillators these equations of motion are exploited for describing a large amplitude collective motion within a locally harmonic approximation.

In the considered range of frequencies the values of the microscopic diffusion coefficients for the inverted and

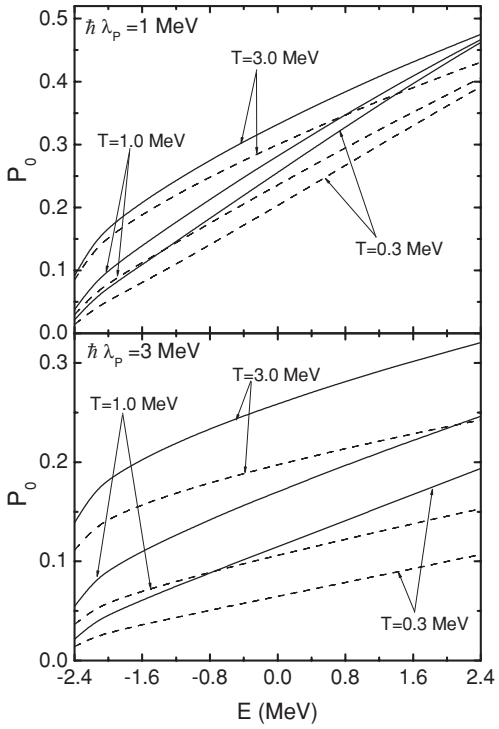

FIG. 11. The calculated asymptotic probability of capture of the Gaussian packet inside of the barrier (the inverted oscillator potential with $\hbar\tilde{\omega} = 1$ MeV) as function of the initial energy $E(0)$ for the indicated temperatures and asymptotic friction coefficients at $\langle R(0)\rangle = -2$ fm, $\sigma_{RR}(0) = 0.42$ fm^2, $\sigma_{PP}(0) = 0.6\hbar^2$ fm^{-2}, $\sigma_{PR}(0) = 0$. The results were obtained with the microscopic diffusion coefficients [Eqs. (21) and (22)] (solid line) and with the phenomenological diffusion coefficient [Eq. (28)] in momentum (dashed line).

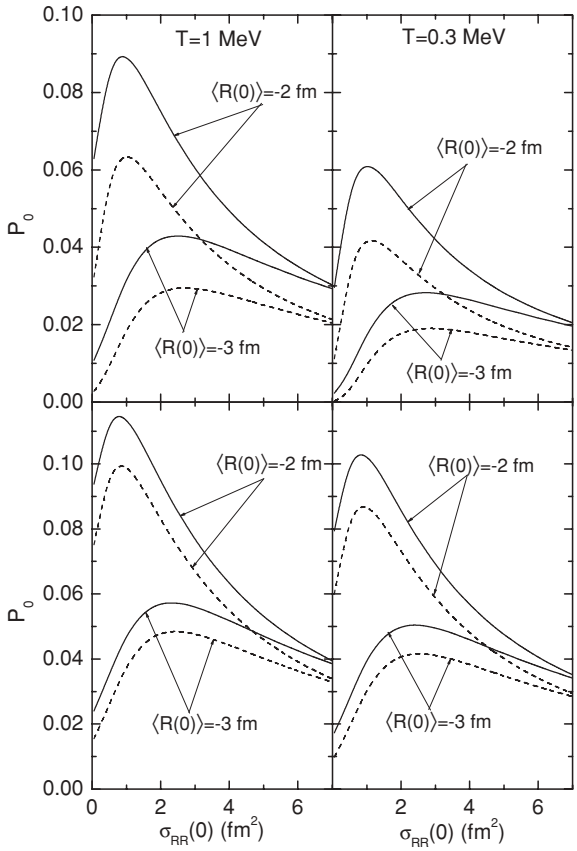

FIG. 12. The calculated asymptotic probability of capture of the Gaussian packet inside of the barrier (the inverted oscillator potential with $\hbar\tilde{\omega} = 1$ MeV) as function of the initial variance $\sigma_{RR}(0)$ in coordinate for the indicated temperatures and initial values of $\langle R(0)\rangle$, and $\sigma_{PP}(0) = 5\hbar^2$ fm^{-2}, $\sigma_{PR}(0) = 0$. The asymptotic friction coefficients are 1 MeV (lower part) and 3 MeV (upper part). The results were obtained with the microscopic diffusion coefficients [Eqs. (21) and (22)] (solid line) and with the phenomenological diffusion coefficient [Eq. (28)] in momentum (dashed line).

harmonic oscillators are close to each other at finite collective frequency and temperature. The difference of diffusion coefficients for negative and positive stiffnesses decreases with increasing temperature. The results demonstrates that there are limitations in applying the microscopical diffusion coefficients to the inverted oscillator below the crossover temperature because at low temperatures the correlation time of the fluctuations of the random forces is comparable or even larger than the characteristic time of the collective subsystem. In this case the modified diffusion coefficients were suggested.

The calculated results showed that via the diffusion coefficients the quantum effects increase with damping. These effects may be quite large at low temperatures. As illustrated, the quantum statistical effects enhance the probability of capture inside of the Coulomb barrier, i.e., the formation of the touching nuclear configuration.

The results obtained prove that the quantum nature of the passing over the barrier should be taken into consideration when one calculates the capture cross section in nucleus-nucleus collisions. As shown, the increase of the passing probability over the barrier with kinetic energy is rather slow, especially for the large friction coefficients. The increase of the passing probability with dissipation was found at energies well below the Coulomb barrier. It could be explained by the fact that at larger friction coefficient the dissipation rate of the energy of collective subsystem is smaller because of smaller kinetic energy and a larger diffusion coefficient in momentum.

The elaborated non-Markovian nonstationary transport coefficients could be applied to the analysis of experiments on nuclear sub-barrier fusion, fission, and binary reaction processes. For example, by solving numerically the master equation for the density matrix, the role of friction, diffusion, and memory effects in the collective dynamics of a quantum system, and in the capture into the potential well can be studied for the anharmonic nucleus-nucleus potential.

ACKNOWLEDGMENTS

This work was supported in part by DFG (Bonn) and RFBR (Moscow).

[1] V. V. Volkov, Phys. Rep. **44**, 93 (1978).

[2] W. U. Schröder and J. R. Huizenga, in *Treatise on Heavy-Ion Science*, edited by D. A. Bromley (New York, Plenum Press, 1984), Vol. 2, p. 115.

[3] P. Fröbrich and R. Lipperheide, *Theory of Nuclear Reactions* (Clarendon, Oxford, 1996).

[4] S. Hofmann and G. Münzenberg, Rev. Mod. Phys. **72**, 733 (2000).

[5] J. Randrup, Nucl. Phys. **A307**, 319 (1978); **A327**, 490 (1979).

[6] P. Fröbrich, Phys. Rep. **116**, 337 (1984); Nucl. Phys. **A545**, 87c (1992); P. Fröbrich and S. Y. Xu, *ibid*. **A477**, 143 (1988).

[7] R. V. Jolos, R. Schmidt, and J. Teichert, Nucl. Phys. **A429**, 139 (1984).

[8] G. G. Adamian, A. K. Nasirov, N. V. Antonenko, and R. V. Jolos, Phys. Part. Nucl. **25**, 583 (1994).

[9] G. Giardina, S. Hofmann, A. I. Muminov, and A. K. Nasirov, Eur. Phys. J. A **8**, 205 (2000).

[10] J. F. Liang *et al*., Phys. Rev. C **75**, 054607 (2007).

[11] M. Beckerman, Rep. Prog. Phys. **51**, 1047 (1984).

[12] M. Dasgupta, D. J. Hinde, N. Rowley, and A. M. Stefanini, Annu. Rev. Nucl. Part. Sci. **48**, 401 (1998).

[13] G. G. Adamian, N. V. Antonenko, W. Scheid, and V. V. Volkov, Nucl. Phys. **A627**, 361 (1997); **A633**, 409 (1998).

[14] G. G. Adamian, N. V. Antonenko, Z. Kanokov, and V. V. Sargsyan, Theor. Math. Phys. **145**, 1443 (2005); Z. Kanokov, Yu. V. Palchikov, G. G. Adamian, N. V. Antonenko, and W. Scheid, Phys. Rev. E **71**, 016121 (2005); V. V. Sargsyan, Yu. V. Palchikov, Z. Kanokov, G. G. Adamian, and N. V. Antonenko, Phys. Rev. A **75**, 062115 (2007); Yu. V. Palchikov, Z. Kanokov, G. G. Adamian, N. V. Antonenko, and W. Scheid, Phys. Rev. E **71**, 016122 (2005); Sh. A. Kalandarov, Z. Kanokov, G. G. Adamian, and N. V. Antonenko, Phys. Rev. E **74**, 011118 (2006); **75**, 031115 (2007).

[15] P. Grigolini and F. Marchesoni, Adv. Chem. Phys. **62**, 29 (1985).

[16] V. M. Kolomietz, S. V. Radionov, and S. Shlomo, Phys. Rev. C **64**, 054302 (2001); V. M. Kolomietz and S. Shlomo, Phys. Rep. **390**, 133 (2004).

[17] S. Radionov and S. Aberg, Phys. Rev. C **71**, 064304 (2005).

[18] H. Hofmann, Phys. Rep. **284**, 137 (1997); H. Hofmann and D. Kiderlen, Int. J. Mod. Phys. E **7**, 243 (1998); C. Rummel and H. Hofmann, Nucl. Phys. **A727**, 24 (2003).

[19] J. H. Weiner, Phys. Rev. **169**, 570 (1968).

[20] P. A. Miller and S. Sarkar, Phys. Rev. E **58**, 4217 (1998).

[21] S. Matsumoto and M. Yoshimura, Phys. Rev. A **63**, 012104 (2000).

[22] Y. Abe, D. Boilley, B. G. Giraud, and T. Wada, Phys. Rev. E **61**, 1125 (2000); J. D. Bao and D. Boilley, Nucl. Phys. **A707**, 47 (2002); D. Boilley, Y. Abe, and J. D. Bao, Eur. Phys. J. A **18**, 627 (2003).

[23] J. D. Bao and Y.-Z. Zhuo, Phys. Rev. C **67**, 064606 (2003).

[24] S. Ayik, B. Yilmaz, A. Gokalp, O. Yilmaz, and N. Takigawa, Phys. Rev. C **71**, 054611 (2005); N. Takigawa, S. Ayik, K. Washiyama, and S. Kimura, Phys. Rev. C **69**, 054605 (2004).

[25] D. Boilley and Y. Lallouet, J. Stat. Phys. **125**, 477 (2006).

[26] J. Ankerhold and E. Pollak, Phys. Rev. E **75**, 041103 (2007).

[27] R. V. Jolos, S. P. Ivanova, and V. V. Ivanov, Sov. J. Nucl. Phys. **40**, 74 (1984); S. P. Ivanova and R. V. Jolos, Nucl. Phys. **A530**, 232 (1991).

[28] V. G. Zelevinsky, in *Proceedings of the XII Winter School the Leningrad Institute of Nuclear Physics* (1977), p. 53.

[29] K. Lindenberg and B. J. West, Phys. Rev. A **30**, 568 (1984).

[30] D. Zubarev, V. Morozov, and G. Röpke, *Statistical Mechanics of Nonequilibrium Processes* (Akademie Verlag, Berlin, 1997); U. Weiss, *Quantum Dissipative Systems* (World Scientific, Singapore, 1999); C. W. Gardiner, *Quantum Noise* (Springer, Berlin, 1991); N. G. van Kampen, *Stochastic Processes in Physics and Chemistry* (North-Holland, Amsterdam, 1981).

[31] G. G. Adamian, N. V. Antonenko, and W. Scheid, Phys. Lett. **A244**, 482 (1998); Phys. Lett. **A260**, 39 (1999); Nucl. Phys. **A645**, 376 (1999); Yu. V. Palchikov, G. G. Adamian, N. V. Antonenko, and W. Scheid, J. Phys. A **33**, 4265 (2000); Physica A **316**, 297 (2002).

[32] G. G. Adamian, R. V. Jolos, and A. K. Nasirov, Phys. At. Nucl. **55**, 366 (1992); G. G. Adamian, A. K. Nasirov, N. V. Antonenko, and R. V. Jolos, Nucl. Phys. **A551**, 321 (1993).